

# Phenomenological model of multiferroic properties in langasite-type crystals with a triangular magnetic lattice

S. A. Pikin\* and I. S. Lyubutin†

*Shubnikov Institute of Crystallography, Russian Academy of Sciences, 119333, Moscow, Russia*

(Received 23 February 2012; revised manuscript received 11 May 2012; published 9 August 2012)

The conditions for occurrence of the magnetoelectric, magnetoelastic, and piezomagnetic effects in crystals of the langasite family with a triangular magnetic lattice are considered on the basis of the phenomenological model. It is shown that the iron-containing langasites with a triangular magnetic lattice may have piezoelectric properties above the Néel temperature  $T_N$ , but they are not ferroelectrics. Occurrence of either ferroelectric or both ferroelectric and piezoelectric states is possible below  $T_N$ , and these crystals can be considered as multiferroics with a helicoid of magnetic moments oriented along the  $c$  axis. The observation of electric polarization  $p_z$  in these crystals at  $T < T_N$  is possible at sufficiently large values of piezocoefficients  $e_{zyz}$  (class 2) or  $e_{zxx}$  (class 3) and as a result of mechanical deformations occurring due to magnetostriction. Moreover, because of magnetoelastic interactions (appearing due to lowering symmetry  $P321 \rightarrow P3$  below  $T_N$ ), the electric polarization and the axis of the magnetic helicoid can both be parallel to the  $z$  axis even in the absence of the Dzyaloshinskii-Moriya (DM) effect. Possible ferroelastic and ferroelectric transitions are considered at  $T < T_N$ . The occurrence of the magnetic helicoid with its axis in the  $ab$  plane is also discussed. It may appear due to the spin-orbit interaction (DM effect). In this case, electric polarization must appear also in the  $ab$  plane.

DOI: 10.1103/PhysRevB.86.064414

PACS number(s): 75.80.+q, 75.50.Ee, 68.35.Rh

## I. INTRODUCTION

In a number of papers<sup>1–14</sup> as well as in the recent reviews<sup>15–18</sup> the magnetoelectric effect has been intensively studied in numerous materials, so-called multiferroics. In particular, Refs. 11 and 13 describe perovskites and Ref. 12 treats the hexagonal  $\text{YMnO}_3$ . Quite recently the langasite family crystals attracted great interest as a new magnetically induced multiferroics. A prototype of langasite is the crystal  $\text{La}_3\text{Ga}_5\text{SiO}_{14}$  known by its wonderful piezoelectric and nonlinear optical properties.<sup>19,20</sup> The substitution of iron ions for gallium in such crystals led to an occurrence of a long-range magnetic order with a complex helicoidal magnetic structure.<sup>21,22</sup> This phenomenon provoked further interest to such materials as to a new type of potential multiferroics.<sup>23–30</sup> Perovskites have different and finely interdependent degrees of freedom and several order parameters which lead to unusual physical phenomena including the effect of colossal magnetoresistance.<sup>5,31</sup> The clear-cut dependence of dielectric properties on a magnetic state is a specific feature of these materials, and a choice of optimal compositions would provide the maximum effects.

Langasites and perovskites differ radically in their structure and temperature-dependent behavior. The electric polarization in langasites appears only below the Néel temperature ( $T_N$ ).<sup>21,27</sup> In some multiferroic perovskites such as  $\text{BiFeO}_3$  and  $\text{BiMnO}_3$  electric polarization occurs because of inherent broken inversion symmetry of these crystals, and that appears at temperatures far above  $T_N$ . However, in the newly discovered multiferroic perovskites  $(\text{Eu}, \text{Y})\text{MnO}_3$ , the electric polarization is induced by the helical spin order that appears only below  $T_N$ . The magnetoelectric effect in these perovskites is revealed as a change (decrease) of spontaneous polarization in a certain temperature range below the magnetic ordering point.<sup>14</sup>

It is found that the orientation of electric polarization relative to crystallographic axes is essentially different in

perovskites and langasites. However, a common property of both types of crystals is a helicoidal twist (torsion) of the magnetic moments which can be considered as magnetic inhomogeneity or frustration (i.e., an incommensurate structure, such as a helical spin arrangement). The helicoid appears along the principal  $c$  axis in langasites<sup>21,22,27,29</sup> and normal to this axis in perovskites, where the appearance of weak magnetism is possible under the application of magnetic field above a threshold value.<sup>14,32</sup> Generally, such a frustration is a common result of absence of the symmetry center in these materials.<sup>5,33</sup>

Previously, it was shown phenomenologically<sup>32</sup> that an applied magnetic field decreases the spontaneous polarization in the  $\text{Eu}_{1-x}\text{Y}_x\text{MnO}_3$  perovskites (due to the Dzyaloshinskii-Moriya effect) and simultaneously increases the magnetic moment of the weak ferromagnetic.<sup>34,35</sup> The magnetic frustration (a helicoidal twist) in langasites is possible without weak ferromagnetism, and the electric polarization occurs along the same  $c$  axis where the wave vector of helicoid is directed.<sup>21,22,27,29</sup> Multiferroics of these types show different temperature behavior below the point of the transition into a magnetically ordered state.

There are a few experimental facts concerning the langasites as multiferroics. The measurements of electric polarization in the  $\text{Ba}_3\text{NbFe}_3\text{Si}_2\text{O}_{14}$  single crystal revealed some indications of the ferroelectric phase transition.<sup>27</sup> The dielectric permeability measurements in this crystal show an anomaly near  $T_N$  when electric field  $E$  was applied normal to the  $c$  axis.<sup>28</sup> The temperature anomaly of permeability near  $T_N$  was also observed in the polycrystalline sample  $\text{Ba}_3\text{SbFe}_3\text{Si}_2\text{O}_{14}$ .<sup>28</sup> The existing experimental data<sup>23–29</sup> give rather contradictory results that are partially explained by the lack of single crystal samples. On the other hand, since the langasites are generally very good piezoelectrics,<sup>19,20</sup> it is also important to elucidate how the deformations, related to the magnetoelastic interaction, can induce the electric polarization. An interesting

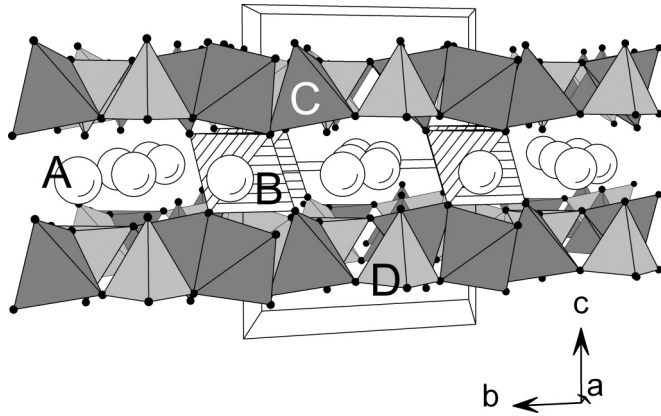


FIG. 1. The trigonal structure of the iron containing langasites with a general formula  $A_3BC_3D_2O_{14}$  (shown on the basis of the  $Ca_3Ga_2Ge_4O_{14}$ -type structure) projected along  $c$  axes. The A and B cations occupy the dodecahedral and octahedral oxygen sites, respectively, and C and D cations are located in the tetrahedral sites. The  $Fe^{3+}$  ions occupy the tetrahedral C sites  $3f$ .

question also arises concerning the nonequivalent sites of iron ions observed in some langasites.<sup>29,30</sup> In particular, it is necessary to understand how this fact correlates with opposite (by sign) rotations of the  $120^\circ$ -packing spins of the triangular magnetic lattice (magnetic chirality) in the  $ab$  plane for different iron sites.

These effects should be theoretically described more precisely, and the aim of this study is the phenomenological definition of the different thermodynamic states of langasites as multiferroics depending on their structure and temperature.

## II. CONDITIONS FOR OCCURRENCE OF THE MAGNETOELECTRIC EFFECT IN LANGASITES

The langasite structure with a general formula  $A_3BC_3D_2O_{14}$  belongs to the trigonal noncentrosymmetrical space group  $P321$  and it is similar to the  $Ca_3Ga_2Ge_4O_{14}$  crystal.<sup>36</sup> The A and B cations occupy the dodecahedral and octahedral oxygen sites, respectively, and C and D cations are located in the tetrahedral sites<sup>19</sup> (Fig. 1). Below the Nèel temperature  $T_N$ , the iron-containing langasites reveal a long-range antiferromagnetic order.<sup>29,30</sup> The moments of  $Fe^{3+}$  cations in C sites ( $3f$ ) form a triangular magnetic lattice in the  $xy$  plane. The magnetic moments of  $Fe^{3+}$  ions in each triangle are oriented at an angle of  $120^\circ$  relative to each other (Fig. 2).<sup>21,28</sup> Moreover, it was shown that this antiferromagnetic phase in langasite  $Ba_3NbFe_3Si_2O_{14}$  gained a helicoidal twist of the iron moments in triangles at their translation along the  $z$  ( $c$ ) axis and, possibly, along a certain axis in the  $xy$  plane.<sup>21,28,29</sup> In this case, the electric polarization  $\mathbf{P}$  oriented along the  $z$  axis also appears,<sup>27</sup> and a presence of its component in the  $xy$  plane is not excluded.<sup>29</sup> Above  $T_N$ , the langasite structure becomes paramagnetic and paraelectric.

### A. The helicoidal magnetic structure and the absence of electric polarization in the triangular magnetic lattice

To understand these phenomena we consider the free-energy  $F$  for a noncentrosymmetric structure.<sup>33</sup> If the magnetic

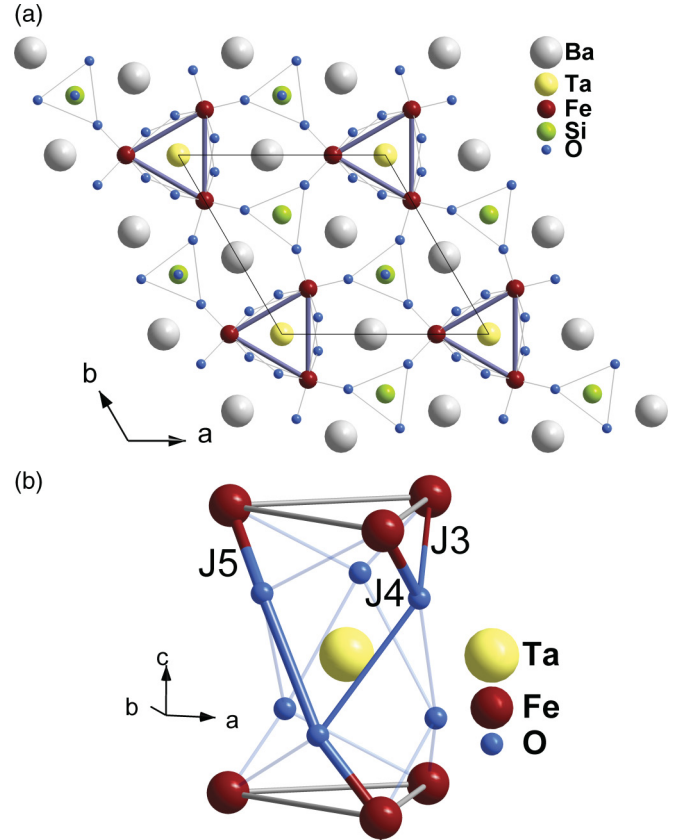


FIG. 2. (Color online) Triangular clusters of  $Fe^{3+}$  ions in the  $a$ - $b$  projection of the trigonal langasite-type structure (by the example of  $Ba_3TaFe_3Si_2O_{14}$ ) shown by solid lines (color blue) (a) and the interlayer superexchange Fe-O-O-Fe interactions  $J_3$ ,  $J_4$ , and  $J_5$  between  $Fe^{3+}$  ions situated in nearest layers (b).

moment  $\mathbf{M}$  of Fe cations is in the  $xy$  plane and it only depends on the coordinate  $z$ , then an invariant in  $F$  exists

$$\begin{aligned} & \alpha [M_x(\text{rot } \vec{M})_x + M_y(\text{rot } \vec{M})_y] + \gamma [(\vec{\nabla} M_x)^2 + (\vec{\nabla} M_y)^2] \\ & = -\alpha (M_x \nabla_z M_y - M_y \nabla_z M_x) + \gamma [(\nabla_z M_x)^2 + (\nabla_z M_y)^2]. \end{aligned} \quad (1)$$

Here  $\alpha$  and  $\gamma$  are the coefficients, and  $\gamma$  is positive. In this case, we can write  $M_x = M \cos(q_z)$  and  $M_y = M \sin(q_z)$ , where  $q_z$  is the wave number. Hence, it follows that minimization of the free-energy  $F$  for a given value  $M$  takes place at  $q_z = -\alpha/2\gamma$ . Appearance of the two components of the magnetization vector  $M_x$  and  $M_y$  indicates that a helicoidal twist of the  $\mathbf{M}$  vectors occurs at the translation along the  $z$  axis. Indeed, the summand in Eq. (1) ( $\vec{M} \text{ rot } \vec{M} = -M_x \nabla_z M_y + M_y \nabla_z M_x = -M^2 q_z$ ) indicates the possibility of spiral twist of the moments in sublattices  $M$  with a nonzero wave number  $q_z$  (Fig. 3). Thus, a helicoidal magnetic structure should appear in any noncentrosymmetric structure below the  $T_N$  point at the finite  $M$  value.

In general, the allowed invariants for various crystals without the center of inversion can involve (dependent on their symmetry) various products of derivatives  $\partial M_i / \partial x_k$  and components  $M_i$ .

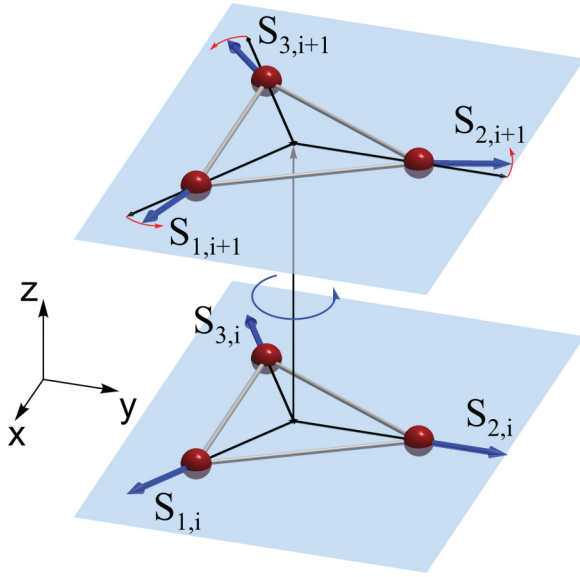


FIG. 3. (Color online) Triangular magnetic lattice of Fe ions with the  $120^\circ$ -spin packing in the plane perpendicular to the  $c$  ( $z$ ) axis. Iron spins  $\mathbf{S}$  in the sublattices 1, 2, and 3 rotate upon translation from the layer  $i$  to the layer  $(i + 1)$  forming a helicoid along the  $c$  ( $z$ ) axis. A rotation of spins in the  $xy$  plane of langasites is shown by the circle arrow.

Furthermore, taking in Eq. (1) the consequent positive expansion terms of the order  $\beta q_z^2 M^4$  into account, one can see that the  $q$  value can change (decrease) with decreasing temperature due to rising of the magnetic moment  $M$ , so

$$q_z = -\alpha/(2\gamma + 2\beta M^2). \quad (2)$$

This characterizes a temperature dependence of a helicoidal structure and indicates that the  $2\pi/q_z$  step of such a translation along the  $z$  axis increases with decreasing temperature, that is, the helicoidal period increases.

Denote the iron moments in the corners of *one* triangle as  $\mathbf{M}_1$ ,  $\mathbf{M}_2$ , and  $\mathbf{M}_3$  ( $\mathbf{M}_i$ ,  $i = 1, 2, 3$ ). These moments are in the basal  $xy$  plane and they are oriented at the angle of  $120^\circ$  relative to each other (Fig. 3). If these moments form spirals at the translation along the  $z$  axis [i.e.,  $M_x = M \cos(q_z z)$ ,  $M_y = M \sin(q_z z)$ , and  $M_z = 0$ ], then it is easy to show that the electric polarization  $P_z$  does not appear in the absence of a summary magnetic moment (antiferromagnetic state), although  $q_z$  may be nonzero. This conclusion can be made if we take into account a summand in the free-energy  $F$  of the form

$$\begin{aligned} \vec{P}[\vec{M} \text{ rot } \vec{M}] &= P_x(M_z \nabla_z M_x) - P_y(M_z \nabla_z M_y) \\ &\quad + P_z(M_x \nabla_z M_x + M_y \nabla_z M_y) \\ &= M_z(P_x \nabla_z M_x - P_y \nabla_z M_y) + \frac{1}{2} P_z \nabla_z M^2 = 0, \end{aligned} \quad (3)$$

where  $M_z = 0$ , and  $M$  is the constant value  $M_i$  in each of the three corners of the triangle.

If all moments  $\mathbf{M}_1$ ,  $\mathbf{M}_2$ , and  $\mathbf{M}_3$  of the triangle deviate out of the  $xy$  plane and form an equal angle with the  $z$  axis (different from  $90^\circ$ ), then a magnetization component  $M_z$  appears along the  $z$  axis (a weak ferromagnetic moment  $\mathbf{m}$ ).

The projections of these moments on the  $xy$  plane retain the  $120^\circ$  orientation. As it follows from Eq. (3), all components of electric polarization  $P_x$ ,  $P_y$ , and  $P_z$  are equal to zero since in this case the sums of the  $M_x$  and  $M_y$  components in the triangle sites of the basal plane are equal to zero. This effect was recently considered in Ref. 9.

Thus, the electric polarization does not appear in the triangular magnetic lattice when twisting magnetization along the  $z$  axis including the case (even in the case) when a nonzero magnetic moment appears along this axis.

### B. The helicoidal magnetic structure and electric polarization in the basal plane

Now suppose that the moments  $\mathbf{M}_i$  of each triangle in the  $xy$  plane retain initial  $120^\circ$  orientation relative to each other, but this orientation can slightly differ in two neighboring triangles of this plane. This may lead to the appearance of a spiral structure along a certain axis  $y'$  lying in this plane. Below we show that at the same initial  $120^\circ$  orientation of  $\mathbf{M}_i$  in the  $xy$  plane, the appearance of electric polarization in the  $xy$  plane is possible due to the Dzyaloshinskii-Moriya (DM) effect.

As it is shown in Fig. 4, all  $\mathbf{M}_i$  moments in the triangle should deviate from the  $xy$  plane at an equal small angle due to the DM effect caused by spin-orbit interaction. The summary magnetic moment of the triangle in the  $xy$  plane remains zero. In this case, the antiferromagnetic ordering in the triangular magnetic lattice is retained, which is only possible at identical projections of the  $\mathbf{M}_1$ ,  $\mathbf{M}_2$ , and  $\mathbf{M}_3$  moments on the  $z$  axis. This forms a summary effect of weak magnetism and an appearance of the moment  $\mathbf{m}$  along the  $z$  axis.

The  $\mathbf{M}_i$  projections on the  $xy$  plane retain their  $120^\circ$  orientation, but now they form a helicoidal spiral in the  $xy$  plane with the axis of the helicoid directed along a certain  $y'$  axis, which is marked by the vector  $\mathbf{r}_{i,i+1}$  in Fig. 4. This vector determines the direction and distance to the nearest neighbor in each sublattice  $\mathbf{M}_i$ . Hence it follows inevitably that the electric polarization  $\mathbf{p}$  occurs along the  $x'$  axis normal to the  $z$  and  $y'$  axes. It must appear due to the spin-orbit interaction

$$\lambda p_{x'} \nabla_{y'} [\vec{S}_i \vec{S}_{i+1}]_z. \quad (4)$$

Here  $\mathbf{S}_i$  is the spin at  $i$  site, and  $\lambda$  is the pseudoscalar parameter of the spin-orbit interaction.  $\vec{e}_j$  are the orthogonal unit axis vectors along the  $x$ ,  $y$ , and  $z$  axes. The parameter  $\lambda$  may be written in the general view as  $\zeta([\vec{e}_1 \vec{e}_2] \vec{e}_3)$ ,  $\zeta$  is scalar,  $|\lambda| = |\zeta|$ . In this case, the DM vector is written as  $\vec{D} = \zeta([\vec{e}_1 \vec{e}_2] \vec{e}_3)[\vec{p} \vec{\nabla}]$ , where  $([\vec{e}_1 \vec{e}_2] \vec{e}_3) \nabla_{y'} [\vec{S}_i \vec{S}_{i+1}]_z = q_{y'} S^2$  and  $q_{y'}$  is the wave vector along the  $y'$  axis.

However, as we show below, the polarization  $p_{x'}$  cannot appear at any temperature below  $T_N$ . This follows from the  $F$  expansion in terms of small values of  $M$ ,  $p_{x'} \equiv p$ , and  $q_{y'} \equiv q$ , which is permitted by the crystal symmetry:

$$F = \frac{1}{2\chi_{e0}} p^2 + bq^4 M^2 + cq^2 M^2 + \frac{1}{2} dp^2 M^2 + \zeta q M^2 p, \quad (5)$$

where the parameters  $b$ ,  $c$ ,  $d$ , and  $\chi_{e0}$  are positive. From Eq. (5) we obtain

$$p \approx -\chi_{e0} \zeta q M^2, \quad q^2 \approx \frac{\chi_{e0} \zeta^2 M^2 - c}{2b}. \quad (6)$$

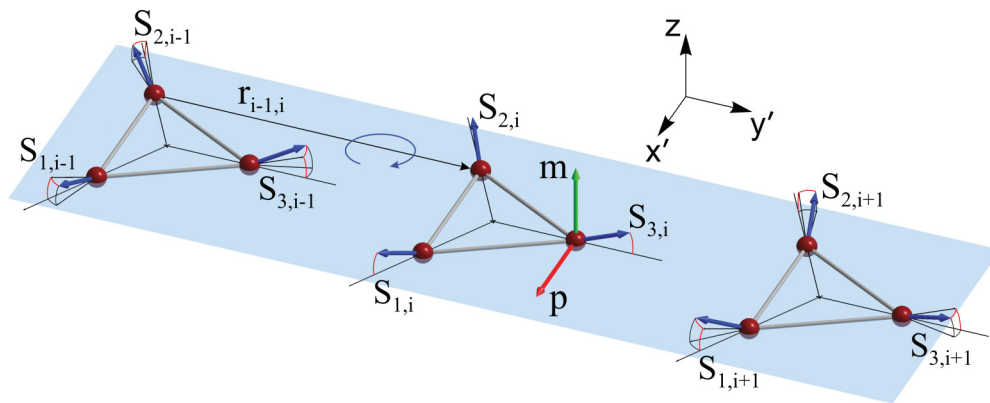


FIG. 4. (Color online) An appearance of the multiferroic state in the triangular magnetic lattice of langasite is shown. Spins  $S$  of the sublattices 1, 2, and 3 forming triangular  $120^\circ$  clusters deviate from the  $xy$  plane at an identical angle due to the DM effect. A weak ferromagnetic moment  $m$  (green arrow) appears along the  $c$  ( $z$ ) axis. Rotation of spins  $S$  upon translation from the cluster  $i$  to the cluster  $(i + 1)$  in the  $xy$  plane leads to a spiral twist of spins along the  $\vec{r}_{i,i+1}$  vectors lying in the  $xy$  plane. A spiral twist of spins is indicated by the circle arrow. The moment value  $m$  in each triangle cluster remains constant at the spiral twist of spins  $S$  in the  $xy$  plane along the  $\vec{r}_{i,i+1}$  vectors. The electric polarization  $p$  (red arrow) perpendicular to both the  $\vec{r}_{i,i+1}$  and  $m$  vectors appears in the  $xy$  plane of such a structure.

It means that the formation of a helicoid of magnetic moments  $M$  in the  $xy$  plane with a wave vector  $q$  calls for the increase of  $M$  below  $T_N$  up to the values of  $M^2 = c/\chi_{e0}\zeta^2$ . Here  $\chi_{e0}$  is the dielectric susceptibility and  $\zeta$  is the modulus of parameter of spin-orbit interaction. Notice that in this case a weak magnetism should be observed along the  $z$  axis.

It follows from Eqs. (5) and (6) that below  $T_N$  the temperature anomaly of the dielectric susceptibility at  $q = 0$  should be observed in the electric field applied along the  $x$  axis. This effect can be observed even in the absence of the spiral twist of magnetic moments. The anomaly may become apparent in an additional decrease of dielectric susceptibility  $\chi_e$  at the increasing in moment  $M$  (i.e., with decreasing temperature). In our approach this follows due to accounting for additional terms of the expansion in  $F$ :  $vp^2 + wp^2M^2$ , then  $\chi_e \sim (v + wM^2)^{-1}$ , where  $w$  and  $v$  are positive phenomenological parameters.

### C. Comparison of the theory with the experimental data

The electric polarization of the  $\text{Ba}_3\text{NbFe}_3\text{Si}_2\text{O}_{14}$  single crystal was measured experimentally in the electric field  $E \sim 50$  kV/cm applied along the  $c$  axis.<sup>27</sup> A sharp increase of the polarization was observed with decreasing temperature below  $T_N$ , and a fast drop of the dielectric constant was also evident. The dielectric permeability in the single crystal  $\text{Ba}_3\text{NbFe}_3\text{Si}_2\text{O}_{14}$  was measured in the alternating field of  $E = 1$  V (with the frequency 100 kHz) applied along and perpendicular to the  $c$  axis.<sup>28</sup> At  $E \perp c$ , the anomaly of permeability near  $T_N$  was found. Below  $T_N$ , the permeability decreases with decreasing temperature. The temperature anomaly of permeability near  $T_N$  was also observed in the polycrystalline sample  $\text{Ba}_3\text{SbFe}_3\text{Si}_2\text{O}_{14}$ ,<sup>28</sup> although crystallites in a powder sample have any arbitrary orientation including an unfavorable one for this effect.

Apparently, the observation of the spiral twist of  $M$  moment along the  $y'$  axis is difficult in compounds of the  $\text{Ba}_3\text{SbFe}_3\text{Si}_2\text{O}_{14}$  type because of a small value of the spin-orbit

interaction parameter  $\lambda$ . Rotation of the polarization vector  $p_x$  under the electric field  $E_z$ , applied along the  $z$  axis, may be difficult in these compounds due to a large electrical anisotropy along the  $x$  axis.

These experimental data confirm our theoretical conclusions reported above. A failure in observation of the polarization  $p_z$  along the  $c$  axis in Ref. 28 is evidently associated with the weakness of the applied electrical field ( $E = 1$  V) necessary for the corresponding displacement of ions.

### III. EFFECT OF MAGNETOELASTIC INTERACTIONS AND VARIOUS MECHANISMS OF ELECTRIC POLARIZATION IN LANGASITES

Displacements of ions responsible for the tensor of deformations  $\hat{u} \sim M^2$  and for the appearance of electric polarization  $p$  may occur below  $T_N$  due to the magnetoelastic interaction. For example, the crystal classes 2 and 3 (the point groups of crystals), in which the coexistence of magnetism and electric polarization takes place, are piezoelectrics. In particular, the described piezoelectric properties connected to the polar tensors of third rank can belong to crystals of 20 classes (the classes 2, 3, 32 admit these properties).<sup>37</sup> It is known that “nonmagnetic” langasites are good piezoelectrics.<sup>20</sup> Particularly, the piezocoefficients  $d_{xyz}$ ,  $d_{zyz}$ ,  $e_{xyz}$ , and  $e_{zyz}$  in class 2 ( $2 \parallel y$ ) are nonzero, so that  $p_x = e_{xyz}u_{yz}$ ,  $p_z = e_{zyz}u_{yz} = d_{zyz}t_{yz}$ ,  $u_{yz} = d_{zyz}E_z$ , where  $u_{ik}$  are the components of the tensor of mechanical deformations  $\hat{u}$  and  $t_{ik}$  is the tensor of mechanical stress.<sup>37</sup>

The piezocoefficients  $e_{zxx}$ ,  $e_{xxx}$ , and  $d_{zxx}$  in class 3 of piezoelectric crystals are nonzero, therefore, the deformation  $u_{xx}$  leads to the value  $p_z = e_{zxx}u_{xx}$ , that is, to the appearance of polarization along the  $c$  axis, and  $u_{xx} = d_{zxx}E_z$ .<sup>37</sup> The deformation  $u_{xx}$  in this crystal class also provokes the polarization  $p_x = e_{xxx}u_{xx}$ . Because of  $\hat{u} \sim M^2$ , the polarization appearing in these classes at  $T \leq T_N$  is proportional to the square of magnetization  $p \sim M^2$ .

If the modulation of magnetic moments appears along the  $y$  axis in the crystal of class 3, then it can be shown that an improper transition by the deformation parameter  $u_{xx}$  occurs. After a substitution of  $p_x = e_{xxx}u_{xx}$  into Eq. (4), we obtain an expression for  $F$  as a function of  $u_{xx}$  which, by analogy with (6), has a minimum at  $u_{xx} = -\zeta e_{xxx}q_y M^2/K$ , where  $K$  is the elasticity modulus. Further minimization of  $F$  leads to a first-order phase transition into a ferroelastic at  $T < T_N$  by the transition parameter  $u_{xx}$  (i.e., by  $q_y$ ). However, because of the DM effect, the temperature of this transition is higher (by the value proportional to  $\zeta^2 e_{xxx}^2 M^2$ ) than the transition temperature into the ferroelastic with the zero  $q_y$  value. Thus, in the crystals of class 3 there is a fundamental property for the formation of electric polarization and magnetization helicity (at  $T < T_N$ , i.e., at  $M \neq 0$ ) in the  $xy$  plane perpendicular to the principal  $z$  axis.

The polarization component  $p_z$  was measured in langasite  $\text{Ba}_3\text{NbFe}_3\text{Si}_2\text{O}_{14}$  in the field  $E$  applied along the  $c$  axis,<sup>27</sup> but the modulation of magnetization with the wave number  $q_y$  and the polarization  $q_x$  in the  $xy$  plane, which are associated with the DM effect, were not studied. In the DM effect, the spiral of magnetic moments and electric polarization cannot appear along the same  $c$  axis when the field  $E$  is applied along this axis. Therefore, we can assert that the nature of polarization  $p_z$  found in  $\text{Ba}_3\text{NbFe}_3\text{Si}_2\text{O}_{14}$  is not associated with the DM effect.

Naturally, if the crystal symmetry decreases  $P321 \rightarrow P3$  (or  $P321 \rightarrow C2$ ), as it is the case of crystals  $\text{Ba}_3\text{NbFe}_3\text{Si}_2\text{O}_{14}$  and  $\text{Ba}_3\text{TaFe}_3\text{Si}_2\text{O}_{14}$  below  $T_N$ , the spontaneous deformation  $u_{xx}$  arises at a proper phase transition when the DM effect is absent, that is, at  $q_y = 0$ . In this case, the polarization is  $p_z = e_{zxx}u_{xx}$ , where the proper transition parameter  $u_{xx}$  appears at the temperature of the transition into a ferroelastic with zero  $q_y$ . However according to Eq. (1), the spiral of magnetic sublattices  $M_i$  exists with a nonzero wave number  $q_z$ . Thus, because of magnetoelastic interactions, the electric polarization and the axis of this magnetic spiral are both parallel to the  $c$  axis in the absence of the DM effect.

The observation of polarization  $p_z$  in  $\text{Ba}_3\text{NbFe}_3\text{Si}_2\text{O}_{14}$  (Ref. 27) and the absence of  $p_z$  in  $\text{Ba}_3\text{SbFe}_3\text{Si}_2\text{O}_{14}$  (Ref. 28) can be explained by the distinction in values of piezocoefficients  $e_{zyz}$  or  $e_{zxx}$  which are different in these materials due to different sizes of Nb and Sb cations. The ionic radius of  $\text{Sb}^{5+}$  is less than that of  $\text{Nb}^{5+}$  and  $\text{Ta}^{5+}$ . The Mössbauer spectroscopy data<sup>30</sup> indicate a noticeable difference in the behavior of the compounds with Sb and with Nb and Ta ions. The transition of  $\text{Ba}_3\text{SbFe}_3\text{Si}_2\text{O}_{14}$  into the ferroelastic should occur at much lower temperature than that in the similar crystals with  $\text{Nb}^{5+}$  and  $\text{Ta}^{5+}$  ions. Finally, a decrease in symmetry  $P321 \rightarrow P3$  with a conservation of the threefold axis in  $\text{Ba}_3\text{NbFe}_3\text{Si}_2\text{O}_{14}$  can provoke a proper transition into the ferroelectric state with a spontaneous polarization  $p_z$ .

Generally speaking, the temperatures of proper transitions into the ferroelectric ( $T_p$ ) or ferroelastic ( $T_u$ ) state do not coincide with the Néel temperature at which the classes with symmetry 2 and 3 appear. The  $T_p$  and  $T_u$  values can be noticeably lower than  $T_N$ . This difference also depends on the radius of large  $\text{Ba}^{2+}$  ions and octahedral  $\text{Sb}^{5+}$ ,  $\text{Nb}^{5+}$ , and  $\text{Ta}^{5+}$  ions which form the layers separating the triangular lattices of the  $\text{Fe}^{3+}$  ions (Fig. 1). The displacements of these cations

along the  $c$  axis cause necessary deformations and polarization due to a magnetoelastic interaction. The polarization  $p_z$  in  $\text{Ba}_3\text{NbFe}_3\text{Si}_2\text{O}_{14}$  sharply increases at  $T_p = 24$  K, whereas  $T_N = 26$  K.<sup>27</sup> It is not difficult to show that when  $T_p < T_N$ , the transition points  $T_p$  and  $T_N$  differ by the value proportional to  $[M(T_1)]^2$ , where  $T_1$  is the point of transition into the ferroelectric state in a nonmagnetic crystal (i.e.,  $T_1 = T_p$  at  $M = 0$ ):

$$T_N - T_p = [M(T_1)]^2 \frac{a'B^2}{b'(a'B + cb')}, \quad T_p = \frac{a'BT_1 + cb'T_N}{a'B + cb'}. \quad (7)$$

Here, a free-energy  $F$  allows the expansion

$$F = a'(T - T_1)p_z^2 + b'(T - T_N)M^2 - cp_z^2M^2 + \frac{A}{2}p_z^4 + \frac{B}{2}M^4. \quad (8)$$

It follows from Eqs. (7) and (8) that  $T_N = T_p$  at  $M(T_1) = 0$ . The polarization is  $p_z = 0$  in the temperature range  $T_p < T < T_N$ .

#### IV. NONEQUIVALENT POSITIONS OF IRON IONS IN SOME LANGASITES AND MAGNETIC AND CRYSTALLOGRAPHIC CHIRALITY

Two nonequivalent positions of  $\text{Fe}^{3+}$  ions were found in the langasite  $\text{Ba}_3\text{TaFe}_3\text{Si}_2\text{O}_{14}$  by the Mössbauer spectroscopy at temperatures below  $T_N$ . It is associated with a structural phase transition induced by the magnetic transition.<sup>29</sup> The structural transition may proceed from trigonal into the monoclinic symmetry (the symmetry decrease  $P321 \rightarrow C2$  with the loss of the threefold axis and retention of the twofold axis) or it may be realized in a crystal class 3 at the symmetry decrease  $P321 \rightarrow P3$  with a retention of the threefold axis. The splitting of  $3f$  sites of  $\text{Fe}^{3+}$  ions into two positions with a common filling equal to unity may occur with their separation from each other by a short distance (0.2–0.5 Å) depending on temperature. A precise refinement of the langasite crystal structure<sup>38,39</sup> indicates that a splitting of the  $3f$  sites takes place at a certain ratio of radii of constituent cations.

The Mössbauer data<sup>29,30</sup> revealed a relatively low (for oxides) value of isomer shift ( $\delta = 0.21$ – $24$  mm/s) in the iron containing langasites which is, evidently, associated with a strong covalence of the chemical bonds Fe-O. This indicates a partial delocalization of the iron  $3d$  electrons, and the  $3d$  shells (nominally  $3d^5$  for  $\text{Fe}^{3+}$ ) may be filled with electrons (or holes) by more or less than half. It is known that such a  $3d$ -shells filling leads to the change in the sign of the spin-orbit interaction parameter  $\lambda$ .<sup>40</sup> This, in turn, results in a change of the sign of the wave number (for example,  $q_z$ ) along the threefold  $c$  axis. This corresponds to opposite (by sign) rotations of the  $120^\circ$ -packing spins of the triangular magnetic lattice (i.e., the change in the sign of chirality) in the  $xy$  plane for different iron positions.

The neutron diffraction data for  $\text{Ba}_3\text{NbFe}_3\text{Si}_2\text{O}_{14}$  (Refs. 21 and 28) established the  $120^\circ$  packing of magnetic moments in each iron triangle on the  $xy$  plane for one type of Fe sites forming a helicoid along the  $c$  axis with a period of about 7 lattice parameters. Apparently, the opposite (in the

chirality sign) helicoids of  $120^\circ$ -spin packing were observed in langasite  $\text{Ba}_3\text{TaFe}_3\text{Si}_2\text{O}_{14}$  for two nonequivalent  $\text{Fe}^{3+}$  sites.<sup>29,30</sup> This is evident from the change in temperature of the angle  $\varphi$  between the iron moment  $\mathbf{M}_i$  and the principal axis of the electric field gradient at a local iron site, which was observed by the Mössbauer effect.<sup>29,30</sup> The temperature dependence of angle  $\varphi \approx \varphi_0 + qr_{i,i+1}$  is associated with the value of magnetic moment  $M$  and it is present in Eq. (2):  $q_z = -\alpha/(2\gamma + 2\beta M^2)$ .

If the  $q$  modulus slightly decreases with increasing  $M$  at temperature lowering, the change in the sign of  $q_z$  may result in both a rise and a decrease of the angle  $\varphi$  value for the nonequivalent iron sites. Such an effect seems to be observed experimentally in Ref. 29. The  $\varphi$  angle difference for two iron sites was much less at low temperatures than at temperatures approaching  $T_N$ . A decrease of  $q_z$  with increasing  $M$  is explained on the basis of Eq. (2). The initial angle values  $\varphi_0$  and the absolute values of wave number  $q_z$  can differ for such nonequivalent sites.

An idea about the connection between magnetic and crystallographic chirality in langasite  $\text{Ba}_3\text{NbFe}_3\text{Si}_2\text{O}_{14}$  was discussed in Refs. 22, 25, 26, 29, 30, and 41. The high sensitivity of helicoidal magnetic structure with respect to the electronic state of cations and their position in crystal lattice was recently demonstrated in the  $\text{Fe}_{1-x}\text{Co}_x\text{Si}$  crystals.<sup>42</sup> It was established that the type of magnetic and crystallographic chirality strongly depends on the Co concentration  $x$ . At  $x \approx 0.2$  the change of the sign of chirality in spin helicoids (from the left hand to the right hand) takes place simultaneously with the sign change in structural chirality. It shows that the sign of DM interaction [the sign of parameter  $\alpha$  in Eq.(1)] is a function of the Fe and Co atoms position, and the electron systems of these atoms interact with the crystal lattice in a different way.

We suppose that the magnetic wave vector  $q_z$  and the structural chirality simultaneously change their signs when the  $3d^n$  shells of the transition elements are filled with electrons (or holes) by more than a half or less than a half.<sup>40</sup> This can be originated at a critical concentration of impurity (cobalt)  $x_0$ . As it is shown in Ref. 42, the absolute value  $|q_z|$  has a maximum at  $x = x_0$ . For instance, at small  $x$ , electrons fill a greater part of the  $3d^n$  shells, so that their total spin is small and the corresponding spin-orbit interaction is weak. With  $x$  changing, electrons are removed from these shells down to the half-shell filling, thus increasing the total spin. The DM parameter  $\alpha$  also increases, but its sign is preserved. In this case, the  $|q_z|$  value increases up to a maximum at  $x = x_0$ . At  $x > x_0$ , the number of holes in these shells increases by more than half, and the total spin and the absolute value of parameter  $\alpha$  decrease (i.e.,  $|q_z|$  decreases). However, at  $x = x_0$ , the sign of  $\alpha$  dramatically changes to the opposite one along with changing in crystallographic chirality because of a mutual rearrangement of atoms, which can be related to the  $3d^n$  shells filling. Phenomenologically, such behavior is described at  $x \approx x_0$  by expression  $|q_z| = q_0 - q'(x - x_0)^2$ , where the parameters  $q_0$  and  $q'$  are positive. We notice that the pitch of helix in  $\text{Fe}_{1-x}\text{Co}_x\text{Si}$  changes with  $x$  from approximately 300 Å to zero. The corresponding maximal rotations of the spins in the basal plane could be estimated from  $\Delta\varphi \approx q_z r \approx 10^{-1}$ . At  $r \approx 5$  Å, the angle between spin directions in the nearest Fe layers is about 10 deg.

We also expect a similar situation in langasites. The helicoidal twisting of magnetic moments of Fe ions, which are in the nonequivalent crystallographic sites, can change its sign in the presence of other atoms (Sb, Ta, Nb, *et al.*) in the octahedral sites separating the Fe layers (Figs. 1 and 2). The character of spin-orbit interactions changes because of a difference in electron orbits and interion distances. The integrals of interplane superexchange interactions Fe-O-O-Fe ( $J_3$ ,  $J_4$ , and  $J_5$  in Fig. 2) can change (decrease) due to the same reason. If these integrals decrease, the rigidity of spin waves can decrease too, and in such a case, the  $|q_z|$  parameter increases at the given temperature. The  $|q_z|$  value decreases with the temperature lowering when the magnetic moment  $M$  increases [see Eq. (2)]. The observable temperature change of the angle<sup>29,30</sup> can be expressed as  $\varphi \approx \varphi_0 + q_z r$  and it originates from the temperature change of the wave number  $\Delta q_z \sim q_z \sim 20 \text{ \AA}^{-1}$ . At  $r \approx 5$  Å (typical for langasites) the corresponding change in the angle is  $\Delta\varphi \sim q_z r \sim 1$  or  $\Delta\varphi \sim 50$  deg which agrees well with the experimental data.<sup>21,28</sup> The signs of  $\Delta\varphi$  values, and correspondingly the signs of  $\Delta q_z$ , are opposite for the nonequivalent Fe sites. This determines the temperature dependence of the helicoidal structure: The step  $2\pi/q_z$ , that is, the pitch of helix, increases at decreasing temperature.

## V. SUMMARY

It is shown that a helicoidal magnetic structure must appear in any noncentrosymmetric structure below the  $T_N$  point (at a finite  $M$  value). The helicoidal period increases with decreasing temperature as the moment  $M$  rises. At the helicoid twist of magnetization along the  $z$  axis, the electric polarization does not appear along this  $z$  axis in the triangular magnetic lattice with a zero moment in the  $xy$  plane. The polarization is also absent when a nonzero magnetic moment appears along this  $z$  axis.<sup>9</sup>

If the helicoidal axis lies in the  $xy$  plane, the electric polarization  $\mathbf{p}$  should appear in the triangular magnetic lattice because of the spin-orbit interaction (DM effect). This polarization is directed along the certain axis  $x'$  perpendicular to the  $z$  and  $y'$  axes (where  $y'$  is the helicoidal axis in the  $xy$  plane). However in this case, the electric polarization does not appear at any temperature below  $T_N$ , but only if the magnetic moment reaches the value  $M^2 = c/\chi_{e0}\zeta^2$ , where  $\chi$  and  $\zeta$  are the material dependent parameters. The available experimental data on the behavior of electric polarization in the iron-containing langasites<sup>27,28</sup> confirm our theoretical conclusions.

Furthermore, we show a possible appearance of electric polarization below  $T_N$  in the crystal classes 2 and 3 due to magnetoelastic interaction. The polarization appears along the different crystal axes depending on the value of piezocoefficients. Thus, in the crystals of class 3 there is a fundamental property for the formation of electric polarization and magnetization helicity (at  $T < T_N$ , i.e., at  $M \neq 0$ ) in the  $xy$  plane perpendicular to the principal  $z$  axis. This effect appears due to the DM interaction.

However, both the electric polarization and the helical axis can also be parallel to the  $z$  axis in the absence of the DM effect

when the magnetoelastic interactions appear upon decreasing symmetry  $P321 \rightarrow P3$  at the Néel point.

In general, the temperatures of the transitions into ferroelectric ( $T_P$ ) or ferroelastic ( $T_u$ ) states do not coincide with the Néel temperature and can be noticeably lower than  $T_N$ . For example, when  $T_P < T_N$ , the transition points  $T_P$  and  $T_N$  differ by the value proportional to  $[M(T_1)]^2$ , and  $T_P = T_N$  at  $M(T_1) = 0$ .

Depending on the filling of  $3d$  shells, the change in the sign of the spin-orbit interaction parameter occurs, which leads to the change in the sign of the wave number  $q_z$  along the threefold  $c$  axis. This corresponds to the opposite (by the sign) rotations of the  $120^\circ$ -spin packing of the triangular lattices

(i.e., the change in the sign of chirality) in the  $xy$  plane for different iron sites. Apparently, such an effect was found in langasite  $\text{Ba}_3\text{TaFe}_3\text{Si}_2\text{O}_{14}$  (Ref. 29) where the temperature-dependent rotation of magnetic moments in opposite directions was observed for two nonequivalent  $\text{Fe}^{3+}$  sites.

#### ACKNOWLEDGMENTS

We thank Dr. K.V. Frolov for his help in the design of the figures. This work is supported by the Russian Foundation for Basic Research Grants No. 11-02-12089 and No. 11-02-00636a and by the Program of the Russian Academy of Sciences “Strongly correlated electronic systems.”

\*pikin@ns.crys.ras.ru

†lyubutin@ns.crys.ras.ru

<sup>1</sup>G. A. Smolenskii and I. E. Chupis, *Usp. Fiz. Nauk* **137**, 415 (1982) [*Sov. Phys. Usp.* **25**, 475 (1982)].

<sup>2</sup>F. Jona and G. Shirane, *Ferroelectric Crystals* (Dover, New York, 1993).

<sup>3</sup>M. E. Lines and A. M. Glass, *Principles and Applications of Ferroelectrics and Related Materials* (Oxford University Press, Oxford, 2001).

<sup>4</sup>N. A. Hill, *J. Phys. Chem. B* **104**, 6694 (2000).

<sup>5</sup>D. I. Khomskii, *Bull. Am. Phys. Soc. C* **21**, 002 (2001).

<sup>6</sup>T. Kimura, T. Goto, H. Shintani, K. Ishizaka, T. Arima, and Y. Tokura, *Nature (London)* **426**, 55 (2003).

<sup>7</sup>T. Kimura, S. Ishihara, H. Shintani, T. Arima, K. T. Takahashi, K. Ishizaka, and Y. Tokura, *Phys. Rev. B* **68**, 060403(R) (2003).

<sup>8</sup>T. Kimura, J. C. Lashley, and A. P. Ramirez, *Phys. Rev. B* **73**, 220401(R) (2006).

<sup>9</sup>M. Mostovoy, *Phys. Rev. Lett.* **96**, 067601 (2006).

<sup>10</sup>S.-W. Cheong and M. Mostovoy, *Nat. Mater.* **6**, 13 (2007).

<sup>11</sup>J. Hemberger, F. Schrettle, A. Pimenov, P. Lunkenheimer, V. Yu. Ivanov, A. A. Mukhin, A. M. Balbashov, and A. Loidl, *Phys. Rev. B* **75**, 035118 (2007).

<sup>12</sup>A. A. Nugroho, N. Bellido, U. Adem, G. Nénert, Ch. Simon, M. O. Tjia, M. Mostovoy, and T. T. M. Palstra, *Phys. Rev. B* **75**, 174435 (2007).

<sup>13</sup>D. I. Khomskii, *Physics* **2**, 20 (2009).

<sup>14</sup>Y. J. Choi, C. L. Zhang, N. Lee, and S.-W. Cheong, *Phys. Rev. Lett.* **105**, 097201 (2010).

<sup>15</sup>A. K. Zvezdin and A. P. Pyatakov, *Phys. Usp.* **47**, 465 (2004).

<sup>16</sup>D. I. Khomskii, *J. Magn. Magn. Mater.* **306**, 1 (2006).

<sup>17</sup>W. Eerenstein, N. D. Mathur, and J. F. Scott, *Nature (London)* **442**, 759 (2006).

<sup>18</sup>K. Zvezdin and A. P. Pyatakov, *Phys. Usp.* **52**, 845 (2009).

<sup>19</sup>B. V. Mill, E. L. Belokoneva, and T. Fukuda, *Russ. J. Inorg. Chem.* **43**, 1168 (1998).

<sup>20</sup>B. V. Mill and Yu. V. Pisarevskiy, in *Proceedings of the 2000 IEEE/EIA International Frequency Control Symposium, Kansas City, Missouri, USA (IEEE) 2000*, p. 133.

<sup>21</sup>K. Marty, V. Simonet, P. Bordet, R. Ballou, P. Lejay, O. Isnard, E. Ressouche, F. Bourdarot, and P. Bonville, *J. Magn. Magn. Mater.* **321**, 1778 (2009).

<sup>22</sup>K. Marty, V. Simonet, E. Ressouche, R. Ballou, P. Lejay, and P. Bordet, *Phys. Rev. Lett.* **101**, 247201 (2008).

<sup>23</sup>M. Kenzelmann, G. Lawes, A. B. Harris, G. Gasparovic, C. Broholm, A. P. Ramirez, G. A. Jorge, M. Jaime, S. Park, Q. Huang, A. Y. Shapiro, and L. A. Demianets, *Phys. Rev. Lett.* **98**, 267205 (2007).

<sup>24</sup>H. D. Zhou, C. R. Wiebe, Y.-J. Jo, L. Balicas, R. R. Urbano, L. L. Lumata, J. S. Brooks, P. L. Kuhns, A. P. Reyes, Y. Qiu, J. R. D. Copley, and J. S. Gardner, *Phys. Rev. Lett.* **102**, 067203 (2009).

<sup>25</sup>C. Stock, L. C. Chapon, A. Schneidewind, Y. Su, P. G. Radaelli, D. F. McMorrow, A. Bombardi, N. Lee, and S.-W. Cheong, *Phys. Rev. B* **83**, 104426 (2011).

<sup>26</sup>J. Jensen, *Phys. Rev. B* **84**, 104405 (2011).

<sup>27</sup>H. D. Zhou, L. L. Lumata, P. L. Kuhns, A. P. Reyes, E. S. Choi, N. S. Dalal, J. Lu, Y. J. Jo, L. Balicas, J. S. Brooks, and C. R. Wiebe, *Chem. Mater.* **21**, 156 (2009).

<sup>28</sup>K. Marty, P. Bordet, V. Simonet, M. Loire, R. Ballou, C. Darie, J. Kljun, P. Bonville, O. Isnard, P. Lejay, B. Zawilski, and C. Simon, *Phys. Rev. B* **81**, 054416 (2010).

<sup>29</sup>I. S. Lyubutin, P. G. Naumov, and B. V. Mill, *Euro Phys. Lett.* **90**, 67005 (2010).

<sup>30</sup>I. S. Lyubutin, P. G. Naumov, B. V. Mill, K. V. Frolov, and E. I. Demikhov, *Phys. Rev. B* **84**, 214425 (2011).

<sup>31</sup>E. Dagotto, *Nanoscale Phase Separation and Colossal Magnetoresistance* (Springer, New York, 2003).

<sup>32</sup>S. A. Pikin, *Crystallogr. Rep.* **56**, 670 (2011).

<sup>33</sup>L. D. Landau and E. M. Lifshits, *Electrodynamics of Continuous Media* (Nauka, Moscow, 1982).

<sup>34</sup>T. Moriya, *Phys. Rev. Lett.* **4**, 228 (1960).

<sup>35</sup>I. Dzyaloshinskii, *Sov. Phys. JETP* **19**, 960 (1964).

<sup>36</sup>E. L. Belokoneva and N. V. Belov, *Dokl. Akad. Nauk SSSR* **260**, 1363 (1981).

<sup>37</sup>I. S. Zheludev, in *Modern Crystallography*, Vol. IV of Physical Properties of Crystals, edited by B. K. Vainshtein (Nauka, Moscow, 1981), p. 153.

<sup>38</sup>A. P. Dudka, Yu. V. Pisarevsky, V. I. Simonov, and B. V. Mill, *Crystallogr. Rep.* **55**, 748 (2010).

<sup>39</sup>A. P. Dudka, R. Chitra, R. R. Choudhury, Yu. V. Pisarevsky, and V. I. Simonov, *Crystallogr. Rep.* **55**, 1060 (2010).

<sup>40</sup>J. B. Goodenough, *Phys. Rev.* **171**, 466 (1968).

<sup>41</sup>M. Loire, V. Simonet, S. Petit, K. Marty, P. Bordet, P. Lejay, J. Ollivier, M. Enderle, P. Steffens, E. Ressouche, A. Zorko, and R. Ballou, *Phys. Rev. Lett.* **106**, 207201 (2011).

<sup>42</sup>S. V. Grigoriev, D. Chernyshov, V. A. Dyadkin, V. Dmitriev, S. V. Maleyev, E. V. Moskvina, D. Menzel, J. Schoenes, and H. Eckerlebe, *Phys. Rev. Lett.* **102**, 037204 (2009).